

Design, Construction, and Testing of a Large-Aperture High-Field HTS SMES Coil

R. Gupta, M. Anerella, P. Joshi, J. Higgins, S. Lalitha, W. Sampson, J. Schmalzle, and P. Wanderer

(Invited Paper)

Abstract—This paper presents the design, construction, and test results of a high-energy-density coil for a superconducting magnetic energy storage system (SMES). The coil was designed to reach 25 T at 4 K in a 100-mm bore under a program funded by ARPA-E. The coil used over 6 km of 12-mm-wide second-generation high-temperature superconductors (HTS) provided by SuperPower. Such high fields and large aperture in a coil built with a new and still-developing conductor and magnet technology created several challenges, which included large stresses and quench protection. This paper summarizes an ambitious research program that resulted in an SMES coil reaching 12.5 T at 27 K. This is the first time that such high fields and such high energy densities have been generated at a temperature over 10 K, and it opens the door for the possible use of HTS magnets in energy storage and other applications.

Index Terms—High-field magnets, HTS, SMES, solenoids.

I. INTRODUCTION

SMES offers a unique solution to energy storage with a potential of providing a large dynamic range, high cycling capability, and excellent energy recovery rate [1]–[6]. Applications include generating rapid pulses, voltage stabilization for improved power quality and potential of grid scale storage [1]–[25]. Several proposals have been made and a few Proof-of-Principle coils have been built [1]–[25]. For example, a 30 MJ SMES coil based on conventional NbTi Low Temperature Superconductor (LTS) was built for the Bonneville Power Authority (BPA) Pacific AC Intertie [1]. However, despite the uniqueness, SMES has not yet been able to make a large impact on the market. The advent of high temperature superconductors and now their availability in increasingly longer lengths offers

an opportunity to revolutionize the field. HTS offers a wide operating range from “high temperature low field” to “high field low temperature.” ARPA-E invited proposals¹ for flexible, large-scale storage for electric grids. A team consisting of ABB, BNL, SuperPower and the University of Houston made a proposal for a “Superconducting Magnet Energy Storage System with Direct Power Electronics Interface” which was funded.² ABB Inc.³ designed and built the power converter and was the project lead; SuperPower [26] manufactured and provided the high strength 2G HTS tape optimized for high fields⁴; the University of Houston developed improved manufacturing techniques for high performance wire; the Condensed Matter Physics & Materials Science Department⁵ at BNL developed the superconducting switch [27]. The Superconducting Magnet Division⁶ at BNL designed, built and tested the SMES coil, developed an advanced quench protection system, low resistance joints for coils and performed the integrated SMES system test. The entire team participated in system integration.

Our initial cost analysis of HTS-based SMES system found that the high field option is significantly less expensive than the high temperature option.^{7,8} Whereas at high fields, the current carrying capacity drops quickly for LTS; it drops very slowly in HTS (Fig. 1). Since the stored energy is proportional to the square of the field, conductor requirement and the system cost would be reduced significantly, if the viability of ultra-high field magnets can be demonstrated. Based on prior work with Particle Beams Lasers, Inc. on high field HTS solenoids [28], BNL proposed the development of a demo module with a high field (~ 25 T) produced in a significant aperture (100 mm) solenoid using the second generation (2G), high strength HTS from SuperPower. Such a magnet is well beyond present technology and posed numerous challenges for the magnet

Manuscript received October 19, 2015; accepted January 10, 2016. Date of publication January 12, 2016; date of current version February 24, 2016. This work was supported in part by the DOE Advanced Research Program Agency-Energy via a Cooperative Research and Development Agreement that BNL has with ABB, Inc. and in part by the Brookhaven Science Associates, LLC under Contract DE-SC0012704 with the U.S. Department of Energy.

R. Gupta, M. Anerella, P. Joshi, J. Higgins, W. Sampson, J. Schmalzle, and P. Wanderer are with the Brookhaven National Laboratory, Upton, NY 11973 USA (e-mail: gupta@bnl.gov).

S. Lalitha is with the Facility for Rare Isotope Beams, East Lansing, MI 48824 USA (e-mail: lalitha@frib.mse.edu).

Color versions of one or more of the figures in this paper are available online at <http://ieeexplore.ieee.org>.

Digital Object Identifier 10.1109/TASC.2016.2517404

¹[Online]. Available: <http://arpa-e.energy.gov/?q=arpa-e-programs/grids>

²[Online]. Available: <http://arpa-e.energy.gov/?q=slick-sheet-project/magnetic-energy-storage-system>

³[Online]. Available: www.abb.com

⁴[Online]. Available: <http://www.tcsuh.com/>

⁵[Online]. Available: <http://www.bnl.gov/cmpmsd/>

⁶[Online]. Available: <http://www.bnl.gov/magnets/>

⁷[Online]. Available: <https://www.bnl.gov/magnets/Staff/gupta/Talks/cca2014/CCA2014-gupta-submitted.pdf>

⁸[Online]. Available: <https://www.bnl.gov/magnets/Staff/gupta/Talks/kyoto2014/Kyoto-2014-gupta.pdf>

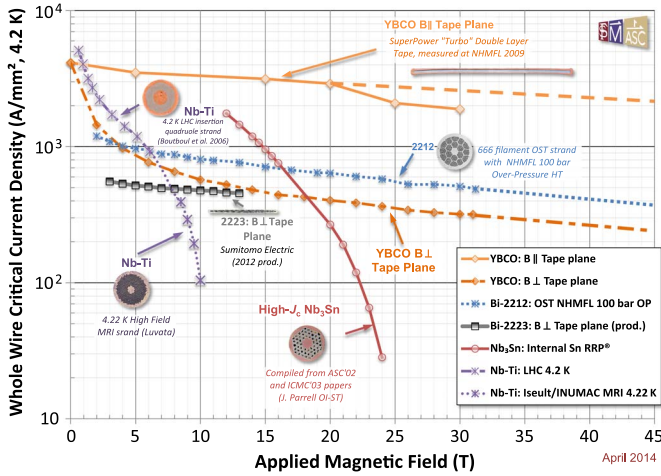


Fig. 1. Engineering current density for various superconductors at 4 K. Data compiled by P. Lee, NHMFL [<http://fs.magnet.fsu.edu/~lee/plot/plot.htm>].

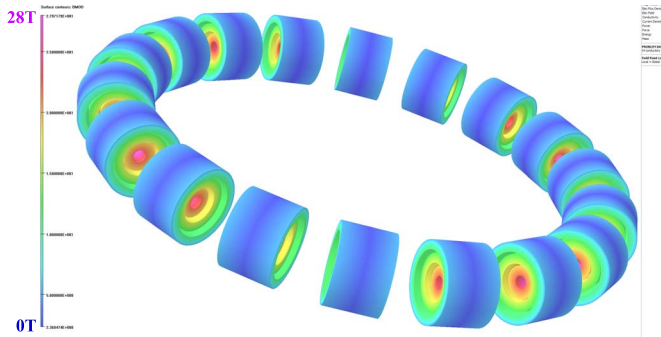


Fig. 2. Toroidal structure containing several modules consisting of HTS pancake coils. Field contours are superimposed over the conductor.

which will be summarized in this paper. The intention of this R&D was to make a large impact rather than just incremental changes. This was also consistent with the “high-risk, high-reward” nature of ARPA-E programs. Even though time and budget limitations allowed only one test, the R&D produced a record field at an attractive temperature in a significant aperture solenoid, which translated into the highest energy density storage device ever produced at a temperature over 10 K. These results exceeded what has been done and even what was ever proposed in any significant SMES proposal. This demonstration opens the potential of the application of HTS magnet technology in the area of energy storage and beyond.

II. SMES COIL DESIGN

The design of the SMES coil consists of several critical components which are described in this section. Quench protection consideration was part of the overall coil design (see Section IV where it is discussed along with the hardware).

A. Overall Design

A grid scale storage device is envisioned to be made of a large number of solenoid modules in a toroidal geometry capable of storing several gigajoules of energy. Fig. 2 shows such a

TABLE I
MAJOR PARAMETERS OF THE 25-T 1.7-MJ ARPA-E SMES COIL

	Quantity	Units
Stored Energy	1.7	MJ
Current	720	Amperes
Inductance	7	Henry
Maximum Field	25	Tesla
Operating Temperature	4.2	Kelvin
Nominal Ramp Rate	1.2	Amp/sec
Nominal width of 2G HTS Tape	12.5	mm
Nominal Thickness of 2G HTS Tape	115, 160	μm
Nominal Thickness of Copper in HTS Tape	55, 100	μm
Nominal Thickness of Stainless Steel Tape	25, 50	μm
Nominal Width of Insulated Double Pancakes	26	mm
Number of Inner Pancakes	28	
Number of Outer Pancakes	16	
Total Number of Pancakes	44	
Inner diameter of Inner Pancake	101	mm
Outer diameter of Inner Pancake	193	mm
Inner diameter of Outer Pancake	223	mm
Outer diameter of Outer Pancake	303	mm
Thickness of Intermediate Support Tube	15	mm
Thickness of Outer Support Tube	7	mm

concept with field contours superimposed over the conductor. Toroidal geometry takes advantage of the fact that the field inside the coil is generally parallel to the surface of the conductor inside the pancake coils where the current carrying capacity is highest (see Fig. 1) and hence the amount of HTS required would be much smaller. As a part of this project we built a demonstration solenoid module made of two layers (inner and outer) of coil with a stainless steel structure in between to keep stresses within the conductor limit. Moreover, the HTS tape was co-wound with Stainless Steel (SS) tape to deal with the high stresses. Major parameters of the demonstration module are given in Table I.

B. Magnetic Design

The magnetic model of the SMES coil consisting of 28 inner pancakes and 16 outer pancakes is shown in Fig. 3. The parameters of the coils are shown in Table I and explained in more detail elsewhere [29], [30]. The outer coil is made shorter in length than the inner coil to reduce the perpendicular component of the field which would be significantly lower in a toroid (Fig. 2) as the end effects will not be present. The thickness of SS tape and the thickness of HTS tape were adjusted to provide grading of the current density (see Fig. 3) to further reduce the perpendicular component of the field, as computed by OPERA [31]. Extra copper in the pancakes in the ends should provide further stability. The maximum computed peak field in the coil at 720 A is ~ 26 T and the maximum perpendicular component ~ 7 T.

C. Mechanical Design

The mechanical structure consists of one inner SS tube, two middle SS tubes (intermediate), one outer tube and two

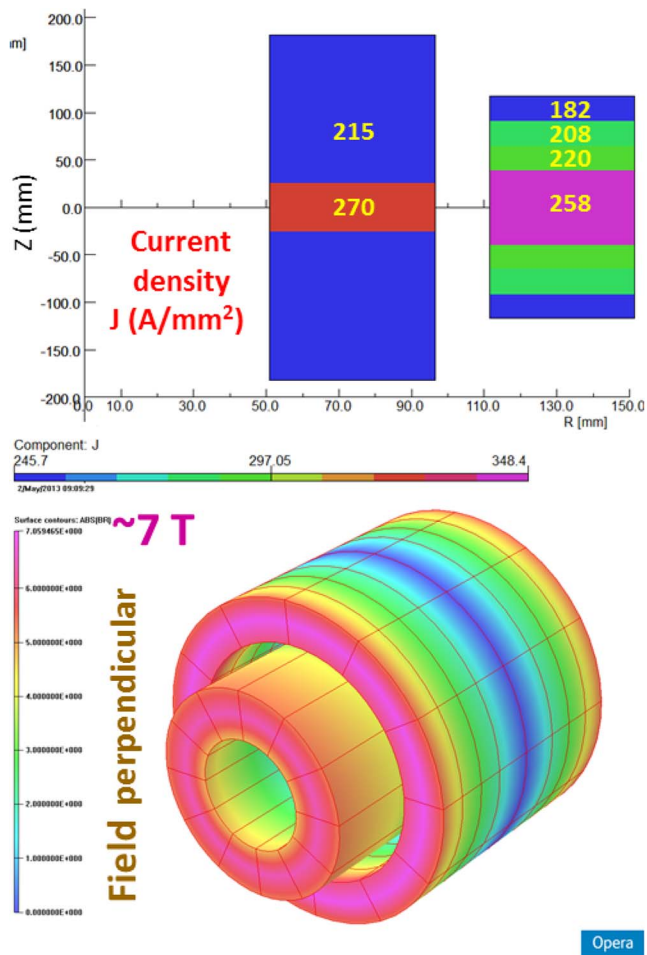


Fig. 3. (Top) 2-D magnetic model of the SMES coil with the contour plot showing the current density. (Bottom) 3-D model with the contour of the perpendicular component of the field superimposed on the surface.

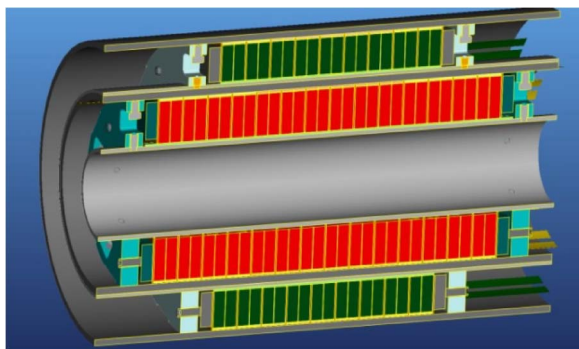


Fig. 4. Basic mechanical model of the SMES structure with inner and outer pancakes, SS support tubes, and end plates.

end plates (see Fig. 4). Use of high strength 2G tape with a Hastelloy substrate was crucial for this application as it allows ReBCO tapes to operate under hoop stress with no degradation. In addition, co-winding HTS tape with SS tape played an important role. A thicker SS tape was used in the pancakes where computed radial forces and hoop-stresses were higher. The coil was designed to maximize the field and stored energy while keeping the stress within 500 MPa and the strain within 0.3%. The axial stress was kept below 120 MPa. These limits

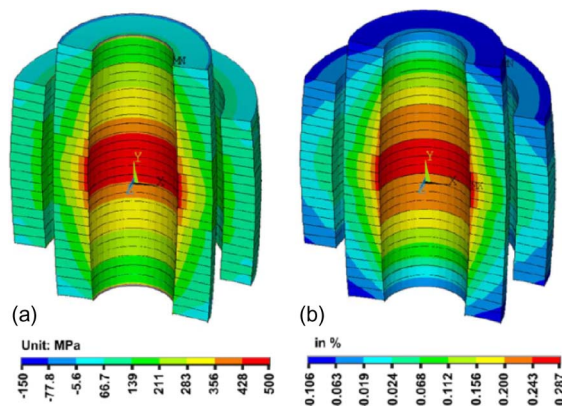


Fig. 5. Contour plots of the (a) hoop stress and (b) hoop strain on the HTS coils [29] performed with ANSYS.



Fig. 6. Computer-controlled universal coil winding machine used for winding inner and outer pancake coils.

were established with the measurements performed earlier on similar conductors [32], [33]. Fig. 5 shows the results of the ANSYS⁹ analysis. The mechanical analysis has been reported in more detail in an earlier paper [29]. Note that the initial model (Figs. 3 and 4) and the analysis (Fig. 5) had 18 pancakes in the outer coil of the magnet, while the actual construction had 16 pancakes (Table I).

III. CONSTRUCTION

Single pancake coils were wound using the computer controlled universal coil winding machine (see Fig. 6). Since the HTS conductor is still in the R&D phase, a number of voltage taps were placed (see Fig. 7) for the 77 K QA test and later removed before the coils are installed inside the magnet structure.

Two single pancake coils were then assembled into a double pancake unit with a spiral splice joint made with similar HTS tape and installed on the inside. The length of the splice joint in the inner pancakes was ~ 15 cm and joint resistance 10 to 16 n Ω (two joints). The length of splice joint in the outer pancake was ~ 20 cm and joint resistance 2 to 8 n Ω [31]. Since the conductor was not available in sufficient length to make pancakes without splices, there were several factory made splices also (typically one in inner pancakes and two in the outer pancakes) with a typical joint resistance of 5 n Ω .

⁹[Online]. Available: www.ansys.com/

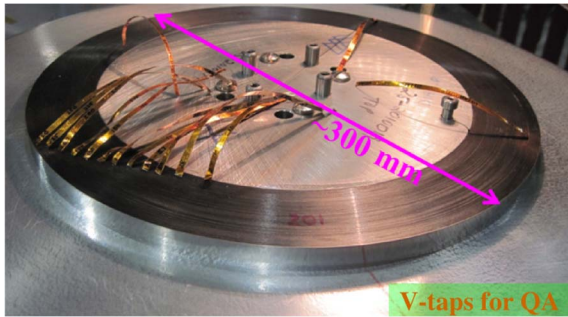


Fig. 7. Outer pancake coil with a number voltage taps.

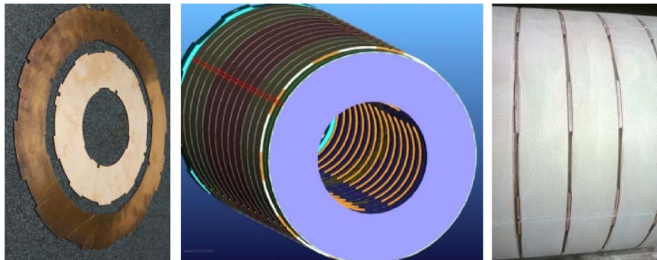


Fig. 8. (Left) Copper discs placed between the inner and outer double pancakes inside the magnet structure (model in the middle and actual construction on right) provide uniform cooling and reduced thermal strain on HTS coils.

Inner and outer coil double pancakes were then stacked onto their respective inner support tubes. Mylar or G10 insulating discs along with the copper discs were installed between double pancakes (see Figs. 4 and 8). Copper discs facilitate uniform cooling and reduce thermal strain on HTS coils. Copper discs are inductively coupled to the coils which help in rapid energy extraction as a part of quench protection.

Double pancakes were then spliced together, individually overwrapped with epoxy impregnated fiberglass tape and cured. Since only one cold test of the system was anticipated given the time and funding restrictions and not all pancakes (wound with R&D conductor) were tested at 4 K, leads were taken out from each double pancake (see Fig. 9) so that the weaker performing pancake (and its corresponding pair to balance the axial Lorentz forces), potentially limiting the performance of the entire system, could be electrically removed without disassembling the entire magnet. Quench protection consideration also dictated the electrical circuit.

After curing, the outer diameters of inner and outer coil assemblies were independently machined to a precise size to provide a close sliding fit to their respective outer support tubes. The support tubes were then installed over the coils and the inner and outer coils were assembled (see Fig. 10) before final lead soldering and instrumentation wiring were completed. At this time the end plates were also installed and engaged to the coil assemblies via set screws to provide axial preload.

IV. QUENCH PROTECTION

Quench protection is a major challenge in HTS magnets, particularly those with large stored energy, because of low quench propagation velocities which could deposit significant energy

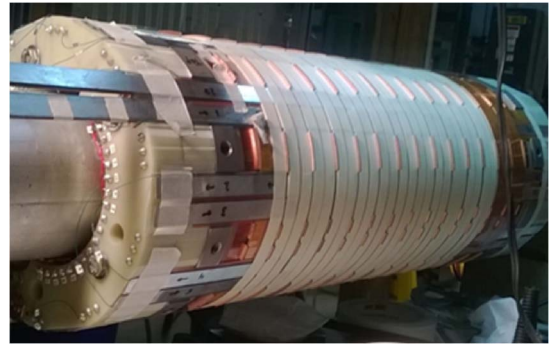


Fig. 9. Inner coil with 28 pancakes, copper discs, voltage taps and leads out from each double pancakes.



Fig. 10. Outer coil with 16 pancakes (top left), inner (bottom left) coil with SS support tube and outer coil with support SS support tube being installed over inner tube (right).

locally causing a permanent damage to the coil. We developed a multi-prong approach consisting of (a) stainless steel (metallic) turn-to-turn insulation for spreading energy faster over a volume, (b) sensitive hardware and software to detect pre-quench phase and act before the thermal runaway takes place, (c) fast energy extraction with electronics that can tolerate high voltage stand-off and (d) inductively coupled copper disks. Quench heaters that have been used in LTS magnets could also be implemented in HTS magnets.

As compared to LTS, there is a relatively long pre-quench phase in HTS, during which the coil can be safely operated with a small resistive voltage. We detect this pre-quench phase and initiate action early on to allow extra time to remove the stored energy.

Quench propagation is significantly different between coils wound with traditional insulations (such as Kapton¹⁰) and those wound with SS tape. Transverse (turn-to-turn) propagation in

¹⁰[Online]. Available: <http://www.dupont.com/products-and-services/membranes-films/polyimide-films/brands/kapton-polyimide-film.html>



Fig. 11. Part of the advanced quench detection electronics system that was specifically developed to have a high sensitivity to detect the onset of the prequench phase at the millivolts or lower level in large coils and tolerate high isolation voltage (over 1 kV) for fast energy extraction.

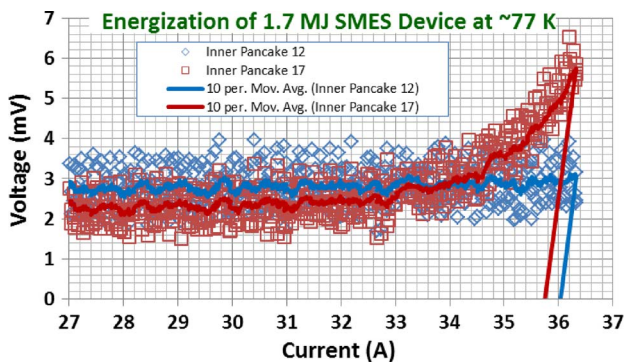


Fig. 12. Detection of the prequench phase and the extraction of energy when a threshold of 2 mV is reached between two pancakes of similar inductances.

coils wound with SS tape is between so called no-insulation [34] and the traditional organic insulation and may be a desired compromise/optimization in some cases, such as in the present application.

Advanced electronics (Fig. 11) were developed [35] (a) to detect a small pre-quench signal (100 μ V to mV level) in the presence of large noise and inductive voltage and (b) to deal with high isolation voltage (< 1 kV), and to allow fast energy extraction in a large stored-energy coil with high inductance. Careful wiring (for example, twisted pairs to reduce noise pick-up), and software development have played a significant role. Numerous voltage taps were used to monitor each pancake and each splice.

One such case is shown in Fig. 12 where a voltage difference of 2 mV between two pancakes while increasing the current triggered shut-off. Even though HTS coils could operate safely at much higher voltage, acting at the mV pre-quench level provides extra time to act to prevent any damage.

The copper discs (Fig. 8), installed initially to provide uniform cooling and reduce thermal strain, played an important role in quench protection. The copper discs are coupled inductively to the coils which helps achieve some almost instantaneous energy extraction. When the current is brought down, it

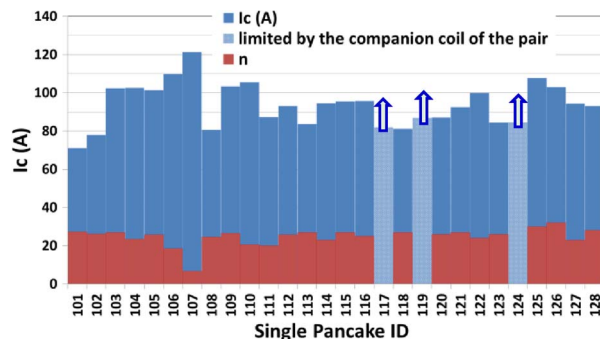


Fig. 13. Histogram of critical current of 28 inner single pancakes at 77 K.

is first transferred from the HTS pancakes to the copper discs before the normal L/R decay (where L is the inductance of the coil and R is the total resistance in the circuit). This strategy (a) removes significant energy quickly, (b) warms up the copper discs and HTS coils (like quench heaters) and (c) gives extra current margin to the coil at the critical time.

Depending on the rate of energy delivery required from the SMES coil for the application, the use of some of the above techniques may however be limited, as they may cause unacceptable losses during the charge-discharge cycle.

V. TEST RESULTS

A large number of tests were carried out as a part of this program. All pancake coils were tested at 77 K. High current/field, low temperature (~ 4 K) tests were performed on a double pancake coil, developmental splice joint, 12 inner coil pancakes, and the fully assembled SMES coil. The test results are discussed briefly below.

A. 77 K Pre-Test of Pancake Coils

Each pancake (inner and outer) was tested at 77 K with a large number of voltage taps (see Fig. 7) to assure that all pancakes perform well individually [30]. This was the most critical part of a series of QA tests instituted before these pancakes were assembled in to the full-size SMES coil. The critical current based on 1 μ V/cm criterion for inner pancakes is shown in Fig. 13. Significant variations in I_c performance of pancakes is attributed to a variation in in-field performance of the conductor. “n” value in Fig. 13 describes the rapidity of transition (see, for example, Fig. 14) of wire or coil from superconducting to non-superconducting state with the expression $V \propto I^n$. Lower “n” in pancake 107 is attributed to a local but acceptable defect in the conductor.

Fig. 14 shows the case when a double pancake coil was not able to pass the QA test. Fig. 14(a) shows the measurement in a good coil and Fig. 14(b) shows the measurement in a defective coil. Incorporation of a large number of voltage taps allows us to identify the section of the conductor with poor performance.

Fig. 15 shows two cases. The case on the left is when the critical currents in two single pancakes were similar and the case on the right is when the critical currents in two single pancakes were significantly different. Both types of double

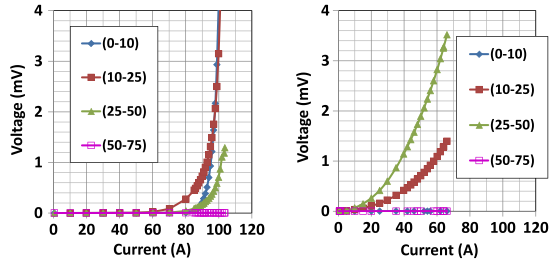


Fig. 14. V-I characteristics of a good coil are shown on the left and of a defective on the right during the 77 K test. Voltage taps help localize the bad region(s) in the coil (see early onset of resistive voltage on the right).

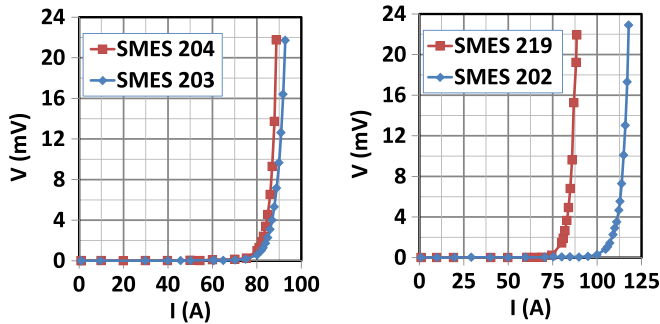


Fig. 15. (Left) Case when two pancakes in the double pancake unit had similar critical currents. (Right) Case when two pancakes in the double pancake unit had significantly different currents.

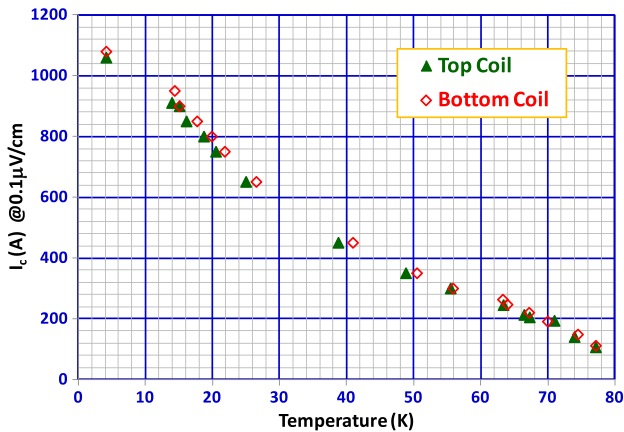


Fig. 16. Critical current as a function of temperature for a double pancake.

pancake units were used in the magnet. It may be pointed out that a high critical current at 77 K does not always correspond to high critical current at 4 K.

B. Double Pancake Coil Test as the Function of Temperature

At the beginning of the program, a double pancake coil was tested at 77 K (liquid nitrogen) and then at 4 K (liquid helium) to ensure that the entire process was reliable before starting the full-scale program. Intermediate temperatures were obtained with gaseous Helium and/or on pumping on nitrogen (60 K to 77 K). All systems (including quench protection and splice joint) worked well to over 1130 Amp. The critical current was measured as a function of temperature during this test (see Fig. 16).

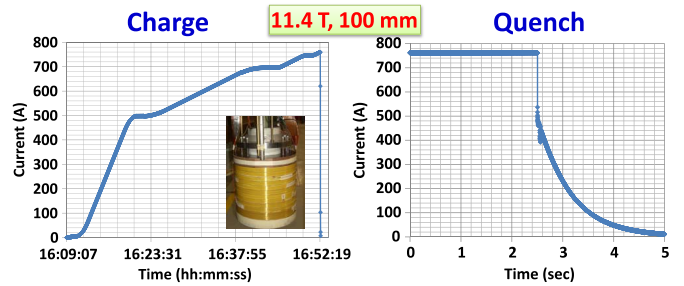


Fig. 17. Quench protection system turned off the power supply and safely extracted the energy when the difference voltage threshold of 2 mV was exceeded.

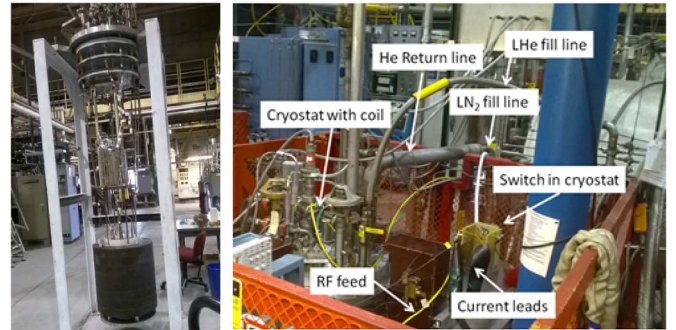


Fig. 18. (Left) Fully instrumented SMES coil on top hat and in Dewar with Switch and (right) other components.

C. Inner Coil 4 K Test

An important milestone was the demonstration of a coil reaching a field of over 10 Tesla with a set of pancakes built for the final magnet. The coil reached 11.4 T field on the axis and 12.1 T on the coil, exceeding the original target of 10 T. The partial coil consisted of 12 pancakes with an inner diameter of 100 mm and an outer diameter of ~ 194 mm. The test run in Fig. 17 shows the coil energized to 760 A at 4 K. Successful quench protection and energy extraction were demonstrated. Maximum internal voltage remained > 1 kV.

D. SMES Coil Test

The fully instrumented SMES coil with iron yoke was installed on the top-hat (Fig. 18(a)) and placed in the Dewar (Fig. 18(b)). The quench protection system with energy extraction, a critical sub-system of the energy storage device, was successfully tested at ~ 77 K at a current of ~ 36 Amp (~ 1.3 T) when 2 mV voltage threshold was reached (Fig. 12).

Before performing the test at full rating—700 Amp (~ 25 T)—at 4 K, a critical current target of 350 Amp (50% of the design current) was set at 20–30 K in Helium gas environment. That goal was successfully reached (Fig. 19) and created a record magnetic field (12.5 T at ~ 27 K).

During this first test campaign, a false signal due to an operator error triggered a power supply shut off and energy extraction at ~ 167 Amp (well below the previous test at 350 Amp) at 35 K (Fig. 19). During this transient, the leads in the inner coil (Fig. 9) were subject to arcing due to excessive voltage.

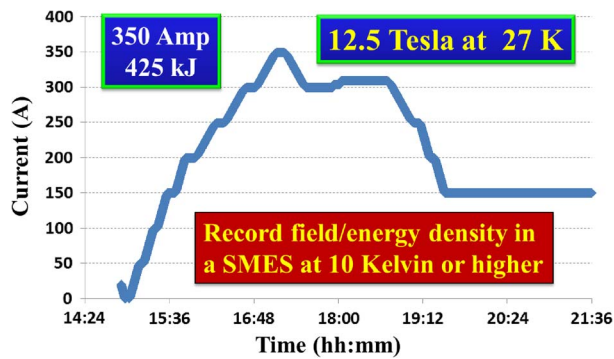


Fig. 19. Record operation of SMES coil reaching 12.5 T at 27 K.

These leads were not part of the baseline design. They were added later in the program for bypassing a potentially weaker performing pancake from limiting the performance of the entire system in the single test allowed within the confines of timeframe and budget. This incident (which occurred after the measurements that are shown in Fig. 19) caused damage to instrumentation, leads and outer turns of a few pancakes of the inner coil. The outer coil appeared to be intact. Following further inspection and low power tests, the area of damage was localized. This may be noted that this arcing is not related to normal magnet construction and does not in any way represent the limit of the high field HTS magnet technology.

E. Integrated System Testing

With little project funds and time left, instead of repairing the coil, ARPA-E SMES program moved towards performing system testing at a low power level. The integrated system test involved the SMES outer coil, quench protection system, superconducting switch [27] and ABB convertor. To protect the overall system, testing was limited to 37 Amps where all components were tested together and limited storage was demonstrated.

VI. CONCLUSION

This paper is a brief summary of the innovative design, engineering, construction, quench protection and test results of a significant SMES program carried out over a short period of about three years. This is the first time that such a large amount of HTS (over 6 km of 12 mm wide tape) has been used in a high field magnet application. The 77 K QA test of HTS coils with a number of voltage taps played an important role. Accidental damage to the lead area does not represent the limit of the HTS magnet technology.

The SMES coil program presented here was a part of an aggressive “high risk, high reward program.” Even though the design goals—high field (25 T), large aperture (~ 100 mm), new conductor (ReBCO), large hoop stresses (~ 400 MPa)—were too aggressive to be achieved in the first attempt, the R&D succeeded in advancing the HTS SMES coil technology well beyond the present state of art. Demonstration of a 12.5 T SMES coil at 27 K, not only is encouraging for energy storage application but for many other areas, as well [36].

ACKNOWLEDGMENT

We thank Qiang Li for initiating this collaboration and providing guidance throughout. Qiang Li and Vyacheslav Solovyov designed and built the superconducting switch. BNL technicians, particularly Glenn Jochen, William McKeon and Ray Ceruti, played key roles. Eric Evangelou worked on HTS program as a high school/undergraduate student and as a part time employee. BNL management provided strong support to the development of the quench protection system and success of the overall program. HTS conductor, feedback and support from SuperPower (particularly from Drew Hazelton) were crucial in achieving positive results. The expertise of Venkat Selvamanickam on HTS conductor was invaluable. We also thank VR V. Ramanan of ABB, who was PI for the SMES project, for his feedback and Eddy Aelozolia who organized various meeting and participated in final integrated testing. Finally, we thank ARPA-E for providing funding for this “high-risk, high reward” R&D.

REFERENCES

- [1] J. Rogers *et al.*, “30-MJ superconducting magnetic energy storage (SMES) unit for stabilizing an electric transmission system,” *IEEE Trans. Magn.*, vol. MAG-15, no. 1, pp. 820–823, Jan. 1979.
- [2] W. Buckles and W. V. Hassenzahl, “Superconducting magnetic energy storage,” *IEEE Power Eng. Rev.*, vol. 20, no. 5, pp. 16–20, May 2000.
- [3] A. P. Malozemoff, J. Maguire, B. Gamble, and S. Kalsi, “Power applications of high-temperature superconductors: Status and perspectives,” *IEEE Trans. Appl. Supercond.*, vol. 12, no. 1, pp. 778–781, Mar. 2002.
- [4] P. Tixador *et al.*, “First tests of a 800 kJ HTS SMES,” *IEEE Trans. Appl. Supercond.*, vol. 18, no. 2, pp. 774–778, Jun. 2008.
- [5] C. A. Luongo, “Superconducting storage system: An overview,” *IEEE Trans. Magn.*, vol. 32, no. 4, pp. 2214–2223, Jul. 1996.
- [6] S. S. Kalsi *et al.*, “HTS SMES magnet design and test results,” *IEEE Trans. Appl. Supercond.*, vol. 7, no. 2, pp. 971–976, Jun. 1997.
- [7] J. H. Bae *et al.*, “Design, fabrication and evaluation of a conduction cooled HTS magnet for SMES,” *Phys. C, Supercond. Appl.*, vol. 469, no. 15–20, pp. 1794–1798, Oct. 2009.
- [8] L. Ottonello *et al.*, “The largest Italian SMES,” *IEEE Trans. Appl. Supercond.*, vol. 16, no. 2, pp. 602–607, Jun. 2006.
- [9] K. Shikimachi *et al.*, “System coordination of 2 GJ class YBCO SMES for power system control,” *IEEE Trans. Appl. Supercond.*, vol. 19, no. 3, pp. 2012–2018, Jun. 2009.
- [10] D. W. Scherbarth, D. T. Hackworth, T. D. Hordubay, O. R. Christianson, and W. V. Hassenzahl, “Design and construction of the 4 tesla background coil for the navy SMES cable test apparatus,” *IEEE Trans. Appl. Supercond.*, vol. 7, no. 2, pp. 840–843, Jun. 1997.
- [11] N. Harada *et al.*, “Development of a 400 kJ Nb₃Sn superconducting magnet for an SMES system,” *Elect. Eng. Jpn.*, vol. 121, no. 3, pp. 44–52, Nov. 1997.
- [12] X. R. Huang, S. F. Kral, G. A. Lehmann, Y. M. Lvovsky, and M. F. Xu, “30 Mw babcock and wilcox Smes program for utility applications,” *IEEE Trans. Appl. Supercond.*, vol. 5, no. 2, pp. 428–432, Jun. 1995.
- [13] H. J. Boenig and J. F. Hauer, “Commissioning tests of the Bonneville Power Administration 30 MJ superconducting magnetic energy storage unit,” *IEEE Trans. Power App. Syst.*, vol. PAS-104, no. 2, pp. 302–312, Feb. 1985.
- [14] M. Ali, B. Wu, and R. Dougal, “An overview of smes applications in power and energy systems,” *IEEE Trans. Sustainable Energy*, vol. 1, no. 1, pp. 38–47, Apr. 2010.
- [15] F. Wang and H. Li, “3-phase current-source SMES-UPS based on TFSC and its control strategies,” in *Proc. IEEE Conf. IPEMC*, Aug. 2006, vol. 1, pp. 1–5.
- [16] M. Ali, T. Murata, and J. Tamura, “Transient stability enhancement by fuzzy logic-controlled SMES considering coordination with optimal re-closing of circuit breakers,” *IEEE Trans. Power Syst.*, vol. 23, no. 2, pp. 631–640, May 2008.

- [17] L. Chen *et al.*, "Detailed modeling of superconducting magnetic energy storage (SMES) system," *IEEE Trans. Power Del.*, vol. 21, no. 2, pp. 699–710, Apr. 2006.
- [18] M. Yamamoto *et al.*, "Development of elementary technologies for 100 kWh/20 MW SMES with multipurpose applications," in *Proc. IEEE Conf. PES Winter Meet.*, Jan. 2004, vol. 4, pp. 2716–2721.
- [19] H. Hayashi *et al.*, "Test results of power system control by experimental SMES," *IEEE Trans. Appl. Supercond.*, vol. 16, no. 2, pp. 598–601, Jun. 2006.
- [20] I. Hassan, R. Bucci, and K. Swe, "400 MW SMES power conditioning system development and simulation," *IEEE Trans. Power Electron.*, vol. 8, no. 3, pp. 237–249, Jul. 1993.
- [21] H. Zhang, P. Liu, K. Dai, Y. Kang, and J. Chen, "DSP controlled chopper in power conditioning system for super-conducting magnetic energy storage," in *Proc. IEEE Conf. IPEMC*, Aug. 2000, vol. 3, pp. 1395–1399.
- [22] N. Celanovic, D. Lee, D. Peng, D. Boroyevich, and F. C. Lee, "Control design of three-level voltage source inverter for SMES power conditioning system," in *Proc. IEEE Conf. PESC*, Jun./Jul. 1999, vol. 2, pp. 613–618.
- [23] D. Peng, D. Lee, F. C. Lee, and D. Boroyevich, "Modulation and control strategies of ZCT three-level choppers for SMES applications," *IEEE Conf. PESC*, Jun. 2000, vol. 1, pp. 121–126.
- [24] A. Arsoy, Y. Liu, P. Ribeiro, and F. Wang, "STATCOM-SMES," *IEEE Ind. Appl. Mag.*, vol. 9, no. 2, pp. 21–28, Mar./Apr. 2003.
- [25] T. Katagiri *et al.*, "Field test result of 10 MVA/20 MJ SMES for load fluctuation compensation," *IEEE Trans. Appl. Supercond.*, vol. 19, no. 3, pp. 1993–1998, Jun. 2009.
- [26] SuperPower Inc., New York, NY, USA. [Online]. Available: info@superpower-inc.com, website: www.superpower-inc.com/
- [27] V. Solovyov and Q. Li, "Fast high-temperature superconductor switch for high current applications," *Appl. Phys. Lett.*, vol. 103, no. 3, Jul. 2013, Art. ID 032603.
- [28] R. Gupta *et al.*, "High field HTS solenoid for a muon collider—Demonstrations, challenges and strategies," *IEEE Trans. Appl. Supercond.*, vol. 24, no. 3, Jun. 2014, Art. ID 4301705.
- [29] S. L. Lalitha and R. C. Gupta, "The mechanical design optimization of a high field HTS solenoid," *IEEE Trans. Appl. Supercond.*, vol. 25, no. 3, Jun. 2015, Art. ID 4601504.
- [30] S. L. Lalitha, W. B. Sampson, and R. C. Gupta, "Test results of high performance HTS pancake coils at 77 K," *IEEE Trans. Appl. Supercond.*, vol. 24, no. 3, Jun. 2014, Art. ID 4601305.
- [31] OPERA Simulation Software, Oxfordshire, U.K. [Online]. Available: vectorfields.info@cobham.com, website: operafea.com/
- [32] W. B. Sampson, M. D. Anerella, J. P. Cozzolino, R. C. Gupta, and Y. Shiroyanagi, "The effect of axial stress on YBCO coils," in *Proc. PAC*, New York, NY, USA, 2011, pp. 1–3.
- [33] W. D. Markiewicz *et al.*, "Design of a superconducting 32 T magnet with ReBCO high field coils," *IEEE Trans. Appl. Supercond.*, vol. 22, no. 3, Jun. 2012, Art. ID 4300704.
- [34] S. Hahn, D. K. Park, J. Bascunan, and Y. Iwasa, "HTS pancake coils without turn-to-turn insulation," *IEEE Trans. Appl. Supercond.*, vol. 21, no. 3, pp. 1592–1595, Jun. 2011.
- [35] P. Joshi, S. Dimaiuta, G. Ganetis, R. Gupta, and Y. Shiroyanagi, "Novel quench detection system for HTS coils," in *Proc. PAC*, New York, NY, USA, Mar. 28–Apr. 1, 2011, pp. 1136–1138.
- [36] R. Gupta *et al.*, "High field solenoid for axion dark matter search at CAPP/IBS," presented at the Conference (MT-24), Seoul, Korea, 2015, Paper 10rAC_05.